pπ-**Molecular Orbitals of Conjugated Linear Polyene Molecules as Molecular Orbital Functional Groups in the Design of Near-infrared Dyes***

Jerry Ray Dias[a,**] *and Gamil A. Guirgis*[b]

[a] *Department of Chemistry, University of Missouri, Kansas City, MO 64110–2499, USA*

[b] *Bayer Corporation, P. O. Box 118088, Charleston, SC 29423–8088, USA*

While reviewing molecular orbital models for the pπ-electronic system of conjugated polyene molecules new examples on embedding of higher linear polyenes will be presented. It is shown that embedding (Hall subgraphs) and right-hand mirror-plane (McClelland subgraphs) fragments are MO functional groups of importance in molecular modeling of near IR absorbing pigments. The major new result reported in this paper is the recognition that the HOMO/LUMO gap for perylene-3,4:9,10-bis(carboximide) and poly(perinaphthalene) related materials is determined by the embedding fragment which circumvents the need to do a full molecule calculation.

Key words: MO functional groups, embedding fragments, right-hand mirror-plane fragments, linear polyenes, HOMO – LUMO, perylene-3,4:9,10-bis(dicarboximide), near IR pigments, poly(perinaphthalene).

INTRODUCTION

Numerous simplifying methods for the evaluation of the pπ-electronic system of polyene molecules has been put forth, and we will briefly review some of these approaches with emphasis placed on a molecular orbital func-

---

* Dedicated to Professor Milan Randić on the occasion of his 70th birthday.

** Author to whom correspondence should be addressed. (E-mail: diasj@umkc.edu)

tional group perspective. We will give several example applications including using perylene related molecules that are chromophore/optical pigment candidates with the goal of designing near-infrared (NIR) absorbing pigments. This latter reduces to finding the structural variables that cause narrowing of the HOMO – LUMO gap of the candidate molecules.

RESULTS AND DISCUSSION

Conjugated polyene molecules are most frequently made up of alternating single and double C-C bonds. Single bonds are referred to as σ-bonds and double bonds contain a σ-bond and a π-bond. All conjugated molecules have a σ-bond backbone of overlapping sp^2 hybrid orbitals. The remaining out-of-plane p_z orbitals on the linking atoms overlap with neighboring p_z orbitals to give π-bonds. Although the chemical structures of these molecules are represented by depictions having alternating single and double bonds, in reality the electrons in the conjugated π-bonds are delocalized over the entire molecule.

The $n \times n$ secular determinant derived from the LCAOs MO theory gives the characteristic polynomial of a molecular graph containing n C atoms. The n roots (eigenvalues) of this n–degree characteristic polynomial are the HMO energies of the associated pπ MOs. We have shown how to write out the characteristic polynomial of any molecular graph with $n \leq 9$ without going through the secular determinant just by counting and identifying the types of vertices and edges of the molecular graph.[1]

Terminology

A molecular graph (G) is a C-C σ-bond skeleton representation of a pπ-conjugated polyene. L_n designates a linear polyene molecule with $n = N$ conjugated carbon pπ centers. $P(G; X) = 0$ designates the characteristic polynomial of a molecular graph G, the roots $[X = (\alpha–E)/\beta]$ of which correspond to the eigenvalues (pπ-electronic energy levels) of G. Thus, L_2 is ethene with the characteristic polynomial of $P(L_2; X) = X^2–1 = 0$ which has eigenvalues of $X = \pm1$. This translates to HMO energy levels of $E = \alpha \pm \beta$.

When two or more molecular graphs have one or more eigenvalues (MO energy levels) in common they are said to be subspectral in those eigenvalues. The more eigenvalues two molecular graphs have in common the more they are similar, particularly if these common eigenvalues include the frontier orbitals (HOMO and LUMO).

It is important to distinguish between alternant and nonalternant hydrocarbons. An alternant hydrocarbon (AH) has no odd size rings. For a mo-

lecular graph of N carbon vertices, let us start with the integer 1 for the index of the most positive eigenvalue X_1, 2 for the second most positive eigenvalue X_2, and so forth going to N for the most negative eigenvalue X_N. For an AH molecular graph, the roots $\{X_k\}$ of the characteristic polynomial $P(G; X)$ appears as pairs

$$X_k + X_{N-k+1} = 0$$

per the pairing theorem. The smallest positive root of $P(G; X)$ corresponds to the pπ-electronic energy in β units of the highest occupied molecular orbital (HOMO) and the smallest negative root corresponds to the lowest unoccupied MO (LUMO).

Embedding Smaller Molecular Graphs onto Larger Ones

Commonly recurring eigenvalues (subspectrality) can be detected by embedding and mirror-plane fragmentation; embedding and right-hand mirror-plane fragments are called Hall and McClelland subgraphs,[2–3] respectively, and are what we regard as MO functional groups. Whenever a smaller molecular graph can be embedded onto a larger one, then the larger one will have the eigenvalues of the smaller one among its eigenvalues. AHs and sometimes alternant subgraphs in an otherwise nonAH can frequently be embedded. Hall's rules[2] for embedding smaller subgraphs onto larger graphs are as follows: i) All vertices connected to the subgraph fragment must be nodes (zero-eigenvector coefficients). ii) On the other side of each of these nodes must be a repetition of the fragment with the opposite sign. iii) Other branches at these nodes will also be nodes. A list of common embedding fragments (or MO functional groups) and their corresponding eigenvectors can be found in several sources.[1] Allyl embedding in 1,2-divinylbenzene and 2,6-dimethylenylstyrene is illustrated in bold in Figure 1.

Figure 1 shows the interrelationships between allyl, 3-methylenyl-4-vinylhexatriene, 1,2-divinylbenzene, 2,6-dimethylenylstyrene, and 1-methylenylnaphthalene all which are subspectral in the eigenvalue pair of $\pm\sqrt{2}$. Both 1,2-divinylbenzene and 2,6-dimethylenylstyrene are doubly degenerate in the eigenvalues of $\pm\sqrt{2}$ because each can be embedded by allyl two distinct ways. Deletion of any vertex from either of these two molecular graphs gives successor molecular graphs having eigenvalues of $\pm\sqrt{2}$ once; deletion of the appropriate vertex from each will give the same successor, 3-methylenyl-4-vinylhexatriene. The eigenvector for the $\sqrt{2}$ eigenvalue is indicated on the molecular graph for 3-methylenyl-4-vinylhexatriene (Figure 1), and it can be seen that joining the appropriate vertices to a zero nodes fulfills the zero-sum rule leading to 1-methylenylnaphthalene. Thus, the embedding re-

sults of Figure 1 explains the origin of the $\pm\sqrt{2}$ eigenvalues in both 3-methylenyl-4-vinylhexatriene and 1-methylenylnaphthalene.
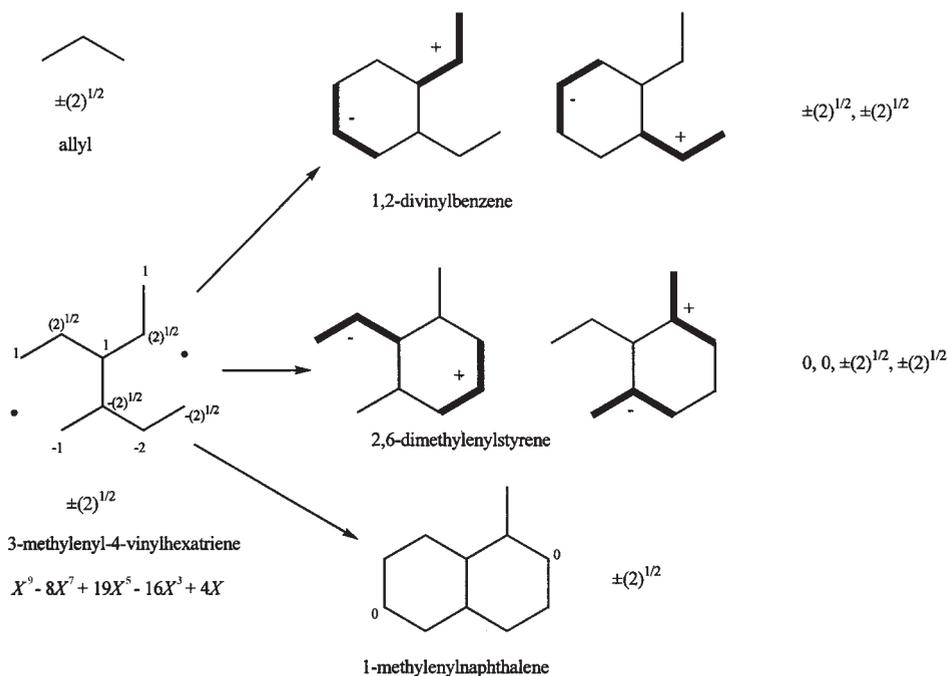

Figure 1. Allyl and 1-methylenylnaphthalene are embedding subgraphs for identifying the presence of the $\pm(2)^{1/2}$ eigenvalues. 1-Methylenylnaphthalene can be derived from 3-methylenyl-4-vinylhexatriene which has $\pm(2)^{1/2}$ eigenvalues by joining its vertices having corresponding eigenvector coefficients of the same magnitude but opposite signs through node vertices as shown above.

Mirror-plane Fragmentation

McClelland's rules[3] for mirror-plane fragmentation are the following: i) The symmetry (mirror) plane divides the molecular graph into right-hand and left-hand fragments. ii) Vertices on the plane of symmetry are included in the left-hand fragment. iii) The weight of the edge between the vertex on the symmetry plane and a vertex in the left-hand fragment is $\sqrt{2}$. iv) Vertices in the right-hand fragment originally connected by a bisected edge have weights of -1 and the opposing vertices in the left-hand fragment have weights of $+1$. v) The eigenvalues of the original molecular graph equal the eigenvalues of the fragment graphs. If a mirror-plane does not bisect any

molecular graph edge, then the right-hand fragment is also a Hall subgraph. The McClelland mirror-plane defines an antisymmetric relationship for the eigenvectors (wave functions) corresponding to the eigenvalues belonging to the right-hand mirror-plane fragments; in this case, any vertices on the mirror-plane have zero eigenvector coefficients. Most of the right- hand mirror-plane fragments (or MO functional groups) having six or less vertices with their eigenvalues and characteristic polynomials have been listed. The mirror-plane fragmentation of 2,6-dimethylenylstyrene gives allyl as the right-hand fragment and is equivalent to the second allyl embedding shown in the middle of Figure 1.

Subspectrality and Dendrimer Polyradicals

Subspectral molecular graphs have one or more eigenvalues in common. If two nearly equal size molecular graphs have a preponderance of eigenvalues in common they are said to be strongly subspectral. The first two molecular graphs in Figure 2 are strongly subspectral.

Dendrimers are star-shaped oligomers and polymers of progressively increasing branching as one moves away from the molecular core center. Polyradical dendrimers are of current interest.[4] Figure 2 presents the smallest triradical, tetraradical, and octaradical molecular graphs that represent ring centrix and vertex centrix core structures for polyradical dendrimers. Both embedding and mirror-plane fragmentation of the molecular graphs in Figure 2 can be performed to show that they possess the eigenvalues of allyl. These molecular graphs have three-fold symmetry and can be embed-
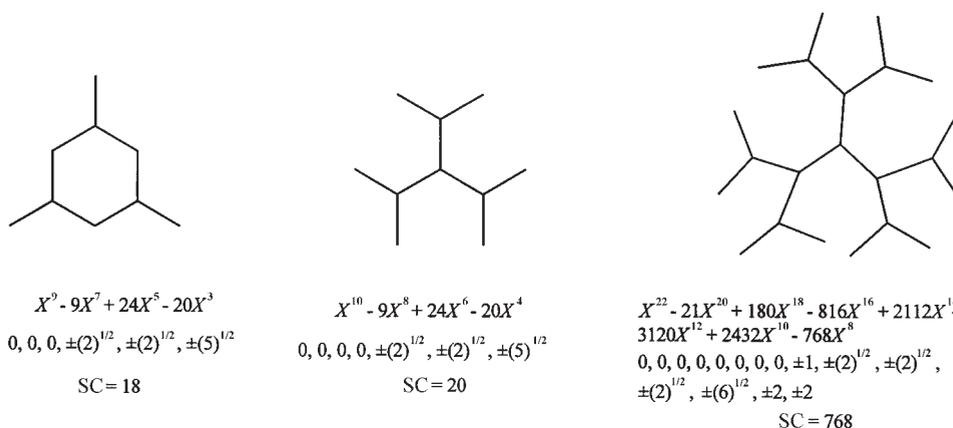

$X^9 - 9X^7 + 24X^5 - 20X^3$

$0, 0, 0, \pm(2)^{1/2}, \pm(2)^{1/2}, \pm(5)^{1/2}$

SC = 18

$X^{10} - 9X^8 + 24X^6 - 20X^4$

$0, 0, 0, 0, \pm(2)^{1/2}, \pm(2)^{1/2}, \pm(5)^{1/2}$

SC = 20

$X^{22} - 21X^{20} + 180X^{18} - 816X^{16} + 2112X^{14} - 3120X^{12} + 2432X^{10} - 768X^8$

$0, 0, 0, 0, 0, 0, 0, 0, \pm1, \pm(2)^{1/2}, \pm(2)^{1/2}, \pm(2)^{1/2}, \pm(6)^{1/2}, \pm2, \pm2$

SC = 768

Figure 2. Dendrimer radicals that can be embedded by allyl (L_3) and their polynomials, eigenvalues. and number of resonance structures (SC).

ded three distinct ways by allyl (L$_3$); only two of these embeddings are mutually independent, and, therefore, it is predicted *a priori* that these molecular graphs must be at least doubly degenerate in the eigenvalues of 0, $\pm\sqrt{2}$.

The corresponding characteristic polynomials are also listed in Figure 2. Since the last two molecular graphs are acyclic, their characteristic polynomials are also matching (acyclic) polynomials and their tail coefficients give the number of resonance structures (SC). The last molecular graph in Figure 2 is the isoconjugate of hexanitroisobutene dianion which is said to be Y-conjugated.[5] Thus the dianion of hexanitroisobutene has 768 resonance structures (SC = 768).

Linear Polyene Molecules

The characteristic polynomials (Chebyshev polynomials) for the linear polyenes are easily obtained by the recursion $P(L_n; X) = XP(L_{n-1}; X) - P(L_{n-2}; X)$ where $P(L_0; X) = 1$ and $P(L_1; X) = X$. For example, $n = 2$ gives $P(L_2; X) = XP(L_1; X) - P(L_0; X) = X^2 - 1 = 0$ for ethene. Using this result gives $P(L_3; X) = X^3 - 2X = 0$ for allyl. Successively repeating this process will generate the characteristic polynomials for all linear polyene molecules.[6]

2-Methylenylpentadienyl has eigenvalues (0, ±1.1756, ±1.9021) that are common to L$_9$ because both give the same left-hand mirror-plane fragment subgraph. Similarly, 2-methylenylhexatriene has eigenvalues (0, ±0.5176, ±$\sqrt{2}$, ±1.9318) common to L$_{11}$ for the same reason; also, 3-methylenylpentadiene has eigenvalues of ±0.5176, ±1.0, ±1.9318.

While embedding of L$_1$ to L$_8$ have been the subject of prior papers,[7] the embedding of L$_9$ to L$_{12}$ will be presented herein for the first time. Embedding of L$_9$ on larger molecular graphs is sparse. L$_9$ itself can be embedded by two L$_4$ units separated by a node vertex. Its eigenvalues of 0, ±1.1756, ±1.9021 have been found in benzo[*f,g*]tetracene. Figure 3 shows that benzo[*c,d*]perylene can be embedded by L$_9$. Both L$_{10}$ and acenaphthylene (C$_{12}$H$_8$) have the same right-hand mirror-plane fragment with eigenvalues of 1.6825, 0.8308, –0.2846, –1.3097, –1.9190 which have corresponding antisymmetric eigenvectors. Embedding of L$_{10}$ in peropyrene (C$_{26}$H$_{14}$, Figure 3) establishes the presence of these eigenvalue pairs (±0.2846, ±0.8308, ±1.3097, ±1.6825, ±1.9190) in the latter. Only one example (Figure 3) of embedding of L$_{11}$ could be found. L$_{11}$ itself can be embedded by two L$_5$ units separated by a node vertex. Both L$_{12}$ and pleiadiene (C$_{14}$H$_{10}$) have the same right-hand mirror-plane fragment with eigenvalues of 1.7709, 1.1361, 0.2411, –0.7092, –1.4970, –1.9419. Embedding of L$_{12}$ in terrylene (C$_{30}$H$_{16}$, Figure 3) establishes the presence of these eigenvalue pairs (±0.2411, ±0.7092, ±1.1361, ±1.4970, ±1.7709, ±1.9419) in the latter. These embedding

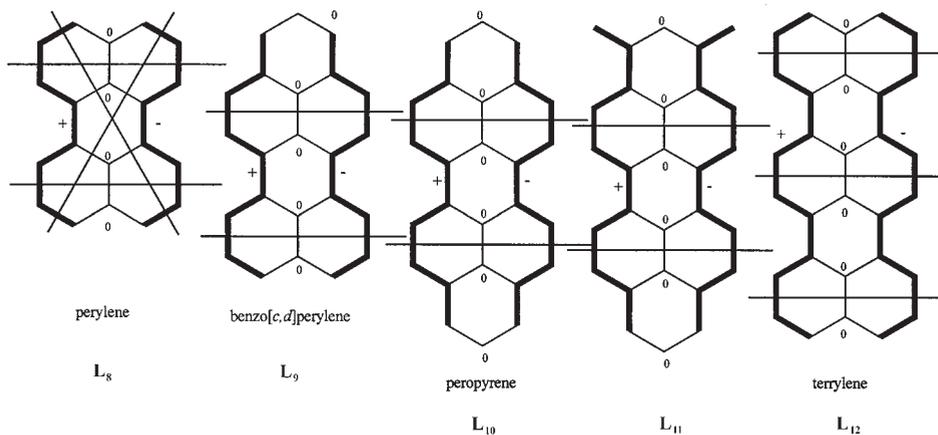fragments are also right-hand mirror-plane fragments of the respective molecular graphs in Figure 3.

Figure 3. Examples of embedding L_8 on perylene, L_9 on benzo[c,d]perylene, L_{10} on peropyrene and L_{11} on its dimethylenyl analog, and L_{12} on terrylene shown in bold with the zero node indicated. Eigenvalues of plus/minus one exist for each line (selective lineation) drawn.

The series in Figure 3 can be extended indefinitely. The infinite member of this series, poly(perinaphthalene), has been the subject of a number of theoretical studies.[8] The main new result reported here is the recognition that the HOMO – LUMO value of any member of this series is given by the corresponding embeddable linear conjugated polyene, *i.e,* poly(perinaphthalene), the limit member, can be embedded by polyacetylene and both have the same band gap value.

The next two nonradical (even carbon) members of the series in Figure 3 (not shown), teropyrene ($C_{36}H_{18}$) and quaterrylene ($C_{40}H_{20}$), have been synthesized,[9] and the former can be embedded by L_{14} and the latter by L_{16}. While these systems as a whole are aromatic, the embedding of linear functional groups determine their HOMO – LUMO gaps. Thus, each of the following pairs have the same HOMO – LUMO values – naphthalene and L_4, pyrene and L_6, perylene and L_8, peropyrene and L_{10}, terrylene and L_{12}, teropyrene and L_{14}, quaterrylene and L_{16}, *etc*. This means that is more economical and facile to determine HOMO – LUMO values for the members of this series by simply computing these quantities for the corresponding embedding functional group. Since the band gap for linear polyenes approaches

zero as they increase in length, the design of new NIR pigments can exploit this simplication.

Perylene-3,4:9,10-bis(dicarboximide)

In this section, we examine the pπ-electronic system of perylene-3,4 : 9,10-bis(dicarboximide) and its derivatives (PTCIs).[10] While PTCIs have been widely used as industrial pigments, laser dyes, photoreceptors in copiers, solar cells, *etc.*, they cannot absorb near-infrared light (NIR), even in the solid state (as pigments). There are two ways of extending the π-conjugation of the perylene chromophore of PTCIs – extension of the perylene framework or arylimide introduction. Arylimide introduction is insufficient to realize NIR absorbing dyes. While the imide substituents do not affect the absorption spectrum of PTCIs, they do control their solid-state color by affecting the intramolecular interaction and crystal packing.[10] To understand how to shift the absorption maximum of the main-band to longer wavelengths toward the NIR region, one needs to understand the structural variables that causes narrowing of the HOMO – LUMO band gap of the candidate pigment molecules.

Figure 4 shows the perpendicular mirror-plane fragmentation of a PTCI. In the first fragmentation, a right-hand fragment which is independent of
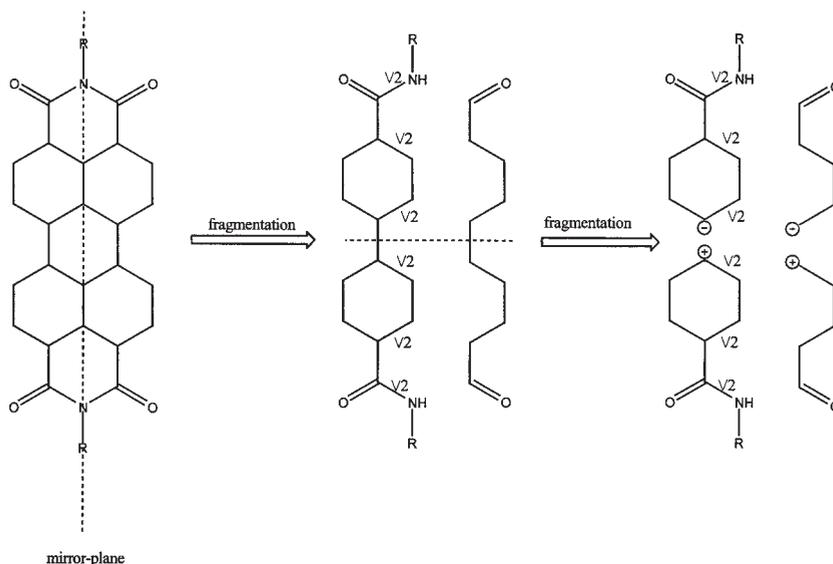

Figure 4. Two perpendicular mirror-plane fragmentations of perylene-3,4:9,10-bis(dicarboximide) (R = H) give four fragments subgraphs.
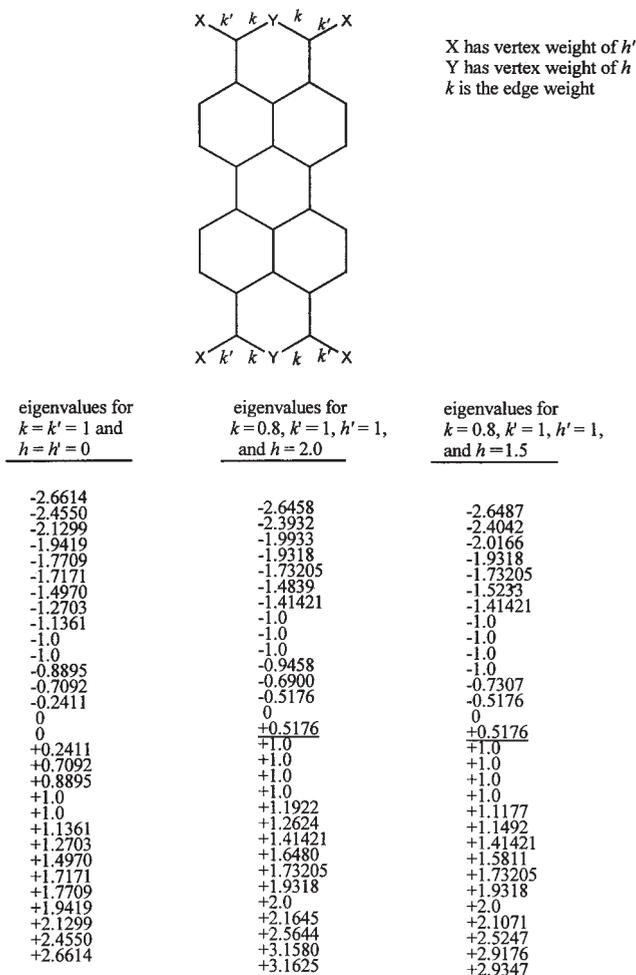
X has vertex weight of h'
Y has vertex weight of h
k is the edge weight

eigenvalues for $k = k' = 1$ and $h = h' = 0$	eigenvalues for $k = 0.8$, $k' = 1$, $h' = 1$, and $h = 2.0$	eigenvalues for $k = 0.8$, $k' = 1$, $h' = 1$, and $h = 1.5$
-2.6614	-2.6458	-2.6487
-2.4550	-2.3932	-2.4042
-2.1299	-1.9933	-2.0166
-1.9419	-1.9318	-1.9318
-1.7709	-1.73205	-1.73205
-1.7171	-1.4839	-1.5233
-1.4970	-1.41421	-1.41421
-1.2703	-1.0	-1.0
-1.1361	-1.0	-1.0
-1.0	-1.0	-1.0
-1.0	-0.9458	-1.0
-0.8895	-0.6900	-0.7307
-0.7092	-0.5176	-0.5176
-0.2411	0	0
0	+0.5176	+0.5176
0	+1.0	+1.0
+0.2411	+1.0	+1.0
+0.7092	+1.0	+1.0
+0.8895	+1.0	+1.0
+1.0	+1.1922	+1.1177
+1.0	+1.2624	+1.1492
+1.1361	+1.41421	+1.41421
+1.2703	+1.6480	+1.5811
+1.4970	+1.73205	+1.73205
+1.7171	+1.9318	+1.9318
+1.7709	+2.0	+2.0
+1.9419	+2.1645	+2.1071
+2.1299	+2.5644	+2.5247
+2.4550	+3.1580	+2.9176
+2.6614	+3.1625	+2.9347

Figure 5. Eigenvalues for 1,3,8,10-tetramethylenylperopyrene, perylene-3,4:9,10-bis-(dicarboxylic) acid dianhydride, and perylene-3,4:9,10-bis(dicarboximide).

the R group is obtained, *i.e.*, it is a MO functional group. This right-hand mirror-plane is also equivalent to an embedding fragment. The consequence of this is that varying the imide R group alters the 18 eigenvalues associated with the left-hand fragment but the 12 eigenvalues associated with the right-hand fragment remain unchanged. This conclusion presumes that the R group itself does not introduce additional pπ-electronic orbital which may result in charge transfer interactions or otherwise overlapping spectral bands. Thus, the optical absorption characteristics and HOMO – LUMO band gap (compare Figure 5 with Figure 6) is controlled by the right-hand

fragment. Solubility and color can be tuned to some degree by varying the imide R group which changes 18 of the 30 eigenvalues, but direct substitution on the perylene nucleus or lengthening the aromatic core will alter all the eigenvalues which should result in a more versatile means of varying HOMO – LUMO and the optical and redox characteristics of these chromophores.
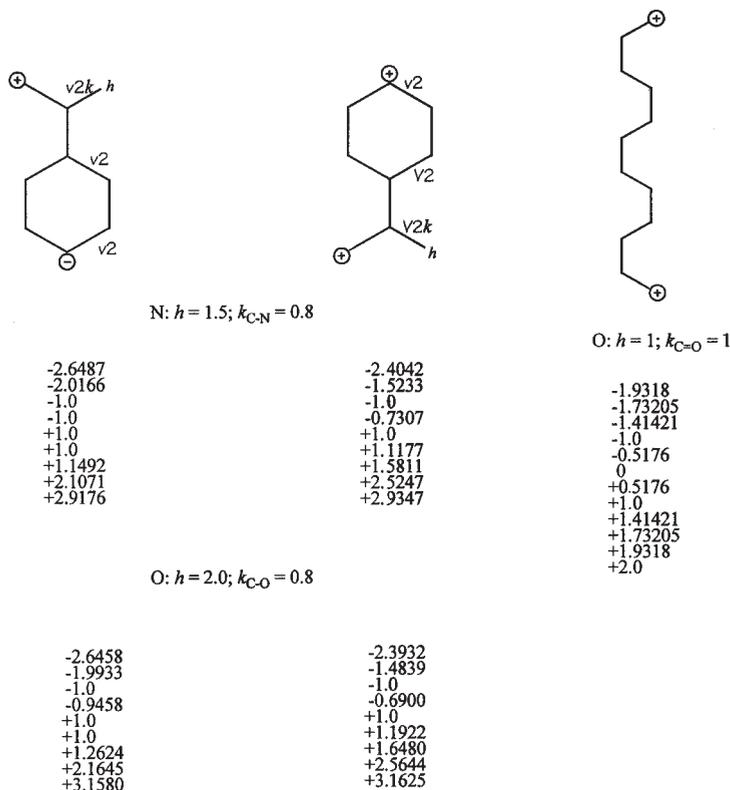

Figure 6. Eigenvalues of parametrized mirror-plane fragments belonging to the molecular graphs in Figure 5. Note that the last fragment is also an embedding fragment and that it contains the frontier energy levels.

In the HMO zero order approximation, the oxygens and nitrogens are replaced by methylenes and methines ($h = 0$ and $k = k' = 1$), respectively. The eigenvalues at this approximation are given in the first column of Figure 5. In the first order approximation, we assign $k = 0.8$, $k' = 1$, $h = 2.0$, $h' = 1$ which models $Y = X =$ oxygen, and this results in the eigenvalues shown in

the second column of Figure 5. Assigning $h = 1.5$ models Y = nitrogen which gives the eigenvalues in the third column. The HOMOs in the second and third columns of Figure 5 are underlined. Comparing the frontier orbitals in the last structure of Figure 5 with the right-hand fragment in Figure 6 shows that the latter controls the HOMO – LUMO gap as previously shown above for the hydrocarbon cores. From these results we expect the $\pi \rightarrow \pi^*$ electronic transitions in the anhydride and imide to be very similar. However, the $n \rightarrow \pi^*$ for the anhydride (Y = oxygen) and imide (Y = nitrogen) will be significantly different because of the energy differences in the lone pair of electrons.

CONCLUSION

In this molecular modeling study, a major strategy for narrowing the HOMO – LUMO band gap to produced potential NIR absorbing pigments has been shown to involve lengthening of the aromatic core structure. The corresponding embedding or right-hand mirror-plane fragment has been shown to be the structural unit which has the major influence on determining the magnitude of the HOMO – LUMO band gap.

REFERENCES

1. J. R. Dias, *Molecular Orbital Calculations Using Chemical Graph Theory*, Springer-Verlag, Berlin, 1993.
2. (a) G. G. Hall, *Trans. Faraday Soc.* **53** (1957) 573–581; (b) *Bull. Inst. Math. Appl.* **17** (1981) 70–72; (c) *J. Math. Chem.* **13** (1993) 191–203.
3. (a) B. J. McClelland, *J. Chem. Soc., Faraday Trans. 2* **70** (1974) 1453–1456; (b) *J. Chem. Soc., Faraday Trans. 2* **78** (1982) 911–916; (c) *Mol. Phys.* **45** (1982) 189–190.
4. (a) A. Rajca, *Chem. Rev.* **94** (1994) 871–893. (b) J. R. Dias, *Z. Naturforsch.* **53a** (1998) 909–918.
5. V. M. Khutoretsky, N. B. Matveeva, and A. A. Gakh, *Angew. Chem., Int. Ed. Eng.* **39** (2000) 2545–2547.
6. J. R. Dias, *Theor. Chim. Acta* **68** (1985) 107–123.
7. J. R. Dias, *J. Chem. Inf. Comput Sci.* **36** (1996) 356–360.
8. (a) M. Randić, *Int. J. Quantum Chem.* **17** (1980) 549–586. (b) D. Bonchev, Ov. Mekenyan, and O. E. Polansky, *Z. Naturforsch.* **36a** (1981) 647–650. (c) D. J. Klein, T. G. Schmaltz, W. A. Seitz, and G. E. Hite, *Int. J. Quantum Chem.* **19** (1986) 707–718. (d) H. Hosoya, H. Kumazaki, K. Chida, M. Ohuchi, and Y.-D. Gao, *Pure & Appl. Chem.* **62** (1990) 445–450. (e) S. Karabunarliev, M. Baumgarten, K. Mullen, and N. Tyutyulkov, *Chem. Phys.* **179** (1994) 421–430.
9. J. R. Dias, *Handbook of Polycyclic Hydrocarbons*, Part A, Elsevier, Amsterdam, 1987.

10. (a) M. Adachi and Y. Nagao, *Chem. Mater.* **13** (2001) 662–669. (b) Y. Zhao and M. R. Wasielewski, *Tetrahedron Lett.* **40** (1999) 7047–7050. (c) U. Rohr, P. Schlichting, A. Bohm, M. Gross, K. Meerholz, C. Brauchle, and K. Mullen, *Angew. Chem., Int. Ed. Eng.* **37** (1998) 1434–1437. (d) D. Desilets, P. M. Kazmaier, and R. A. Burt, *Can. J. Chem.* **73** (1995) 319–324. (e) D. Desilets, P. M. Kazmaier, R. A. Burt, and G. K. Hamer, *Can. J. Chem.* **73** (1995) 325–335.

SAŽETAK

pπ-Molekulske orbitale konjugiranih poliena koje služe kao molekulsko-orbitalne funkcijske skupine u modeliranju pigmenata nižega infracrvenog spektra

Jerry Ray Dias i Gamil A. Guirgis

Dan je pregled molekulsko-orbitalnih (MO) modela π-elektronskih sustava konjugiranih poliena i novi primjeri uklapanja viših linearnih poliena. Pokazano je da su uklapajući fragmenti (tzv. Hallovi podgrafovi) i fragmenti koji zakreću zrcalnu ravninu u desno (tzv. McClellandovi podgrafovi) važne MO funkcijske skupine u molekulskom modeliranju pigmenata nižega infracrvenog spektra. Glavni rezultat ovoga rada je da je razlika HOMO-LUMO kod perilena-3,4:9,10-bis(karboksimida), poli(perinaftalena) i srodnih tvari određena uklapajućim fragmentom, pa se tako zaobilazi račun za cijelu molekulu.